J Solid State Electrochem (2000) 4: 273–278

ORIGINAL PAPER

Michał Grdeń · Jan Kotowski · Andrzej Czerwiński

The study of electrochemical palladium behavior using the quartz crystal microbalance

II. Basic solutions

Received: 10 August 1999 / Accepted: 24 September 1999

Abstract The electrochemical quartz crystal microbalance (EQCMB) method has been used to evaluate the processes which occur in/on the palladium electrode in basic solutions. Hydrogen electrosorption in palladium is accompanied by an additional frequency shift that can be attributed to the stresses generated inside the Pd metal. A non-linear dependence between the mass change and the charge consumed during hydrogen oxidation in the Pd electrode has been found for hydrogen absorbed in the α- and β-phases. This effect precludes the objective estimation of the amount of hydrogen absorbed inside the Pd electrode. The EQCMB method has been used, however, for studying the surface electrode processes on the Pd electrode, i.e. specific anion adsorption, surface oxidation and dissolution. Also, the structure of the palladium oxide formed on the Pd surface during electrochemical oxidation is discussed in this paper and the effect of the anodic limiting potential on the oxide structure is reported.

Key words Palladium · Hydrogen sorption · Surface oxides · Electrochemical quartz crystal microbalance

Introduction

The electrochemical quartz crystal microbalance (EQCMB) offers a unique possibility for measuring in situ the weight changes accompanying electrochemical processes which occur in or on electrodes. The EQCMB method has been already used for the investigation of hydrogen electrosorption in palladium [1–11]. It was demonstrated that the strains inside the metal, created during the hydrogen sorption process, also change the frequency response of the EQCMB crystal [1, 5–8, 10, 11]. In this way the EQCMB response is not equal to the electrode mass changes only. On the basis of our EQCMB results, obtained for the hydrogen sorption process in the Pd electrode in acidic solutions [11], we have postulated that these stresses change in a non-linear manner with the amount of absorbed hydrogen during the electrode saturation with hydrogen, both in the α- and β- phases. We have concluded from the EQCMB results that this effect precludes the objective estimation of the amount of hydrogen sorbed inside the palladium electrode. We also presented experimental data which showed that, during the cyclic changes of the potential of the Pd electrode in acidic solutions, the palladium metal dissolves into the solution. These dissolution results are in good agreement with other data obtained previously [12]. A scheme for the dissolution reaction of the surface oxides involving the exchange of anions from the solution into the surface layer during the surface oxidation/reduction processes has been proposed.

Based on the previous results discussed above, our main conclusion, concerning the use of the EQCMB method, is that this method is more convenient for studying the electrode surface processes, i.e. specific anion adsorption on electrode surface, electrode dissolution or electrode surface oxidation/reduction processes, than investigating hydrogen sorption in the bulk of the palladium metal.

This paper deals with the study of the behavior of the palladium electrode in basic solutions compared to the acidic solutions [11]. Both EQCMB and cyclic voltammetry techniques were used and the limited volume palladium electrodes (Pd-LVE [11, 13–17]) were applied in this work.

Experimental

The EQCMB instrumentation is of the same type as used by Koh et al. [18] and was made in the Institute of Physical Chemistry of

M. Grdeń · J. Kotowski · A. Czerwiński (✉)
Department of Chemistry, The University of Warsaw,
Pasteura 1, 02-093 Warsaw, Poland

A. Czerwiński
Industrial Chemistry Research Institute,
Rydygiera 8, 01-793 Warsaw, Poland

the Polish Academy of Sciences in Warsaw. 5 MHz quartz crystals (AT-cutting) with 12.5 mm diameter (Phelps), covered with a layer of gold and then with a thin layer of palladium, have been used as working electrodes. Palladium thin layers (ca. 200 nm) were deposited on gold from an ammonia-palladium chloride bath at a constant current density (ca. 5 mA cm^{-2}). Deposition efficiency (above 90%) was estimated, in each experiment, from the EQCMB measurements. Platinum gauze and silver-silver chloride electrodes were used as the auxiliary and reference electrodes, respectively. All potentials presented in this paper were recalculated and are referred to the SCE electrode. Current-potential curves were recorded using a potentiostat (Elpan EP 20 A) and a linear sweep generator (Elpan EG 20) coupled with an IBM compatible computer via an ADC/DAC converter (Ambex LC-011-1612). Frequency measurements were made with a Hewlett-Packard HP 53131A universal counter coupled with the computer. EQCMB calibration was performed in 10^{-3} M $AgNO_3$ in 0.1 M $HClO_4$ solution according to the procedure described in detail by Koh et al. [18] and the sensitivity was 10.47 ng Hz^{-1}. The solutions (0.1 M KOH) were prepared with triply distilled water and purity grade reagents. Before the experiments the solutions were deaerated by passing argon through the solution, and during the measurements the gas was directed above the solution surface. Cyclic voltammetry was used as an electrochemical method and the amount of hydrogen sorbed into palladium was calculated from the hydrogen oxidation wave, recorded during the positive potential scan after electrode saturation at a fixed cathodic potential [13, 16, 17]. Theoretically, mass changes during the reaction can be calculated directly from the frequency changes Δf (mass $= \Delta f \cdot s$, where s is the sensitivity in mass per frequency units), while the number of moles of electrons passed during the same reaction is calculated from the charge q (i.e. $q \cdot F^{-1}$, where F is Faraday constant). In this way, the $\Delta f \cdot s \cdot F \cdot \Delta q^{-1}$ value is expressed in molar mass units (g mol^{-1}). However, very often this value is not equal to the real molar mass of the species involved in the reaction. The reason might be that more than one species might participate in the whole charge transfer reaction and/or some additional species are exchanging from the solution. In the latter case, the mass change is equal to the difference of the masses of the species involved in the exchange process (mass of electrode increases or decreases), while in the former case the mass change calculated for one mole of reacting species is the average value for all the species existing on the electrode surface. Nevertheless, the $\Delta f \cdot s \cdot F \cdot \Delta q^{-1}$ value can be the source of important information about the processes occurring during the electrode reactions. In this paper, the $\Delta f \cdot s \cdot F \cdot \Delta q^{-1}$ value is called the "apparent molar mass" (M_a).

Results and discussion

During hydrogen sorption and desorption processes into palladium, the mass of the electrode increases or decreases, respectively. In this experiment, hydrogen was sorbed at a constant potential for the time necessary for full electrode saturation. Because the amount of hydrogen absorbed into the electrode depends on its potential [11, 13–17, 19–23], different electrode saturations with hydrogen were obtained when the electrode was polarized at various potentials [11]. After completing the saturation, the hydrogen oxidation peak was recorded during the positive CV scan (sweep rate 10 mV s^{-1}). The amount of hydrogen sorbed in the palladium electrode was calculated from the integration of this positive anodic peak [11, 13–17, 22]. The dependence of the frequency changes (Δf) on the charge of the oxidized hydrogen (Q_{oxH}), obtained during hydrogen desorption, is presented in Fig. 1. This dependence, Δf vs. Q_{oxH},

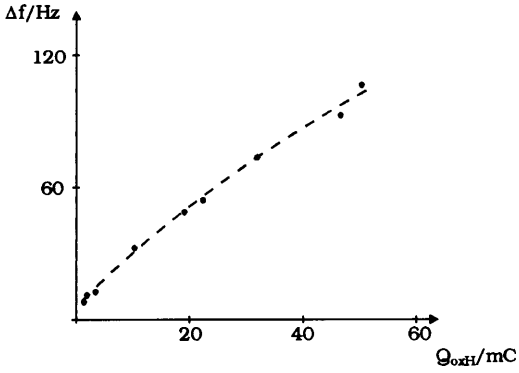

Fig. 1 Dependence of Pd electrode mass changes (Δf) on charge (Q_{oxH}) passed during oxidation of absorbed hydrogen. Solution 0.1 M KOH, sweep rate 10 mV s^{-1}

obtained in basic solutions, is non-linear and it is similar to the one obtained earlier in acidic solutions [11]. Therefore, the ratio $\Delta f/Q_{oxH}$, which is directly proportional to the "apparent molar mass", M_a, depends on Q_{oxH} and decreases with the hydrogen saturation increase in the thin layer palladium electrode (Fig. 2).

Figure 2 demonstrates the changes of the M_a values with the amount of charge needed for hydrogen desorption (Q_{oxH}). Theoretically, the ratio M_a should be close to one (hydrogen atomic mass) in the whole range of the absorbed hydrogen, but experimental values differ from this value both when the α-phase is generated and when the β-phase exists. The M_a value estimated in the β-phase presence is ca. three times lower than the M_a value observed for the α-phase. The same effect was observed in acidic solution [11], where the apparent molar mass calculated from gravimetrical data for hydrogen dissolved in the α-phase was also higher than the values obtained for the β-phase. These effects are due to the strains inside palladium, generated by absorbed hydrogen, and have been reported and discussed in detail in the literature [1, 6–8, 10]. The value of the apparent molar mass, M_a, calculated for hydrogen in the β-phase absorbed from basic solution, is close to the value obtained in acidic solution [11], but more

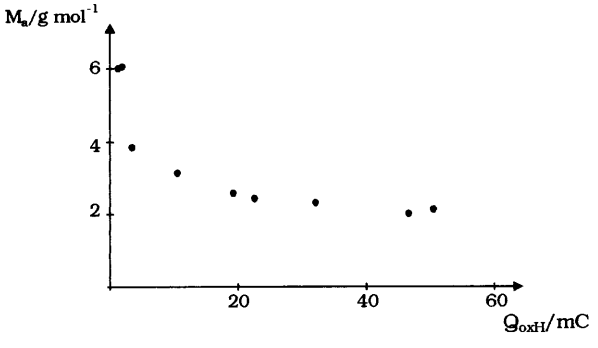

Fig. 2 Dependence of apparent molar mass (M_a) of desorbed hydrogen calculated from oxidation process on charge of oxidation of absorbed hydrogen (Q_{oxH}). Solution 0.1 M KOH, sweep rate 10 mV s^{-1}

significant differences exist in the region of the α-phase. The values of M_a obtained in basic solutions for the α-phase are ca. two times higher than those found in acidic solution. It has to be noted that for low hydrogen concentration, i.e. the α-phase, the values of M_a are less reproducible than in the β-phase both in basic and acidic solutions.

The differences in M_a values, obtained during absorption in basic and acidic solutions in the presence of the hydrogen α-phase, might be caused by two effects: alkali metal intercalation from basic solution into the Pd electrode [13–15, 24, 25] and adsorption of anions on this electrode.

Figure 3 presents both current and EQCMB frequency changes during the cyclic voltammetry of the Pd electrode obtained over a wide potential range, i.e. in the full hydrogen-oxygen potential range. The shape of the CV curve is typical for the Pd electrode in basic solutions [13–15, 23, 26–29]. The mass increase and decrease during hydrogen absorption and desorption, respectively, are clearly visible in the hydrogen sorption-desorption region. Contrary to the results obtained in acidic solution [11], in basic solution the frequency-potential curve is closed, i.e. after finishing the full cycle of the electrode polarization, the value of the frequency returns to its previous value at the beginning of the potential cycling (Fig. 3). This means that there are no irreversible changes of the mass of the electrode. Therefore, it is obvious that palladium dissolution in basic solution is below the detection limit of the microbalance used in this work, and it is much lower than that observed in acidic solution [29–31].

During the negative scan (Fig. 3), two increases of the frequency, i.e. two decreases of mass, are observed. The first one starts at a potential of ca. 250 mV and the second one is visible at ca. −300 mV. The former frequency change corresponds to the beginning of the wide and poorly defined peak. This process is better visible on the frequency-potential curve (frequency change ca. 2 Hz). The latter mass change is coupled with a well-defined reduction peak in the potential range from ca. −150 to ca. −450 mV. The potential of this peak is shifted towards negative values with increase of the anodic potential limit of the polarization of the palladium electrode. This effect was also observed by other authors [29]. These two decreases of mass correspond to the reduction of two different surface oxides.

During the positive scan, only one mass increase is observed after desorption of all absorbed hydrogen and it corresponds to the process of surface oxidation.

During the positive potential scan, the charge passed during surface oxidation (Q_{ox}) and corresponding frequency changes (Δf) can be calculated from the CV and EQCMB curves, respectively. The Δf vs. Q_{ox} plot is presented in Fig. 4. In the calculations, the double layer charges were not subtracted. The reason was that in the potential region, where the surface oxidation of noble metals occurs, the value of a double layer capacity is not constant [32, 33]. It can be seen from this plot that at the point indicated by the arrow, i.e. at $E_i \approx 200$ mV, a change of the Δf vs. Q_{ox} slope occurs. For the potentials higher than E_i, this slope is lower than that observed for the lower potentials. This result indicates that, at the E_i potential, changes occur in the mechanism of the palladium surface oxidation and/or in the surface oxide composition as well its structure.

Further information about the structure of the surface oxide was obtained from CV experiments, in which

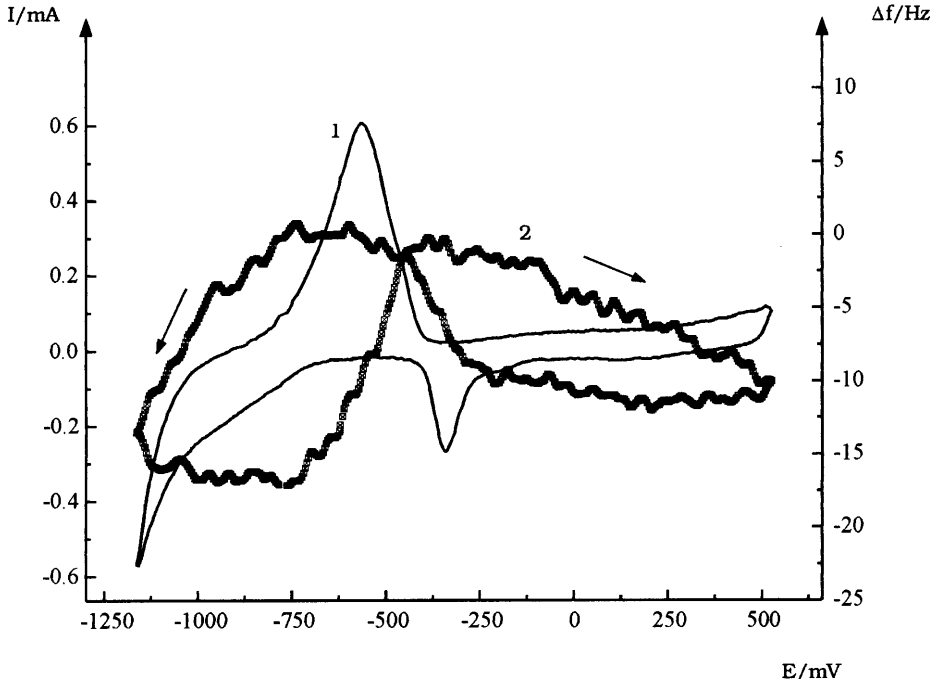

Fig. 3 Cyclic voltammetry curve (*1*) and corresponding electrode frequency changes (*2*) for palladium electrode. Solution 0.1 M KOH, scan rate 25 mV s^{-1}

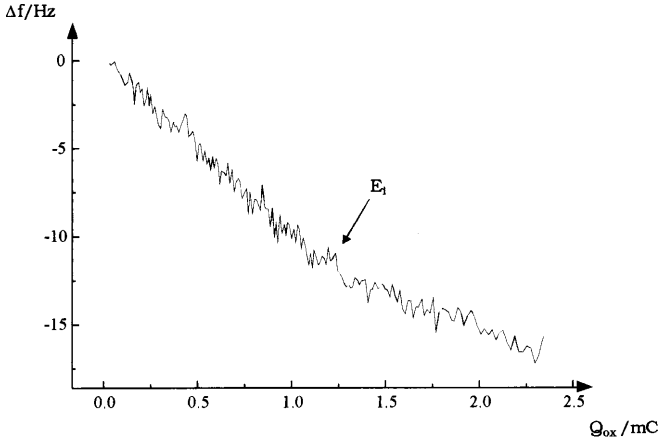

Fig. 4 Dependence of Pd electrode frequency response (Δf) on charge passed during surface oxidation (Q_{ox}). Solution 0.1 M KOH, scan rate 25 mV s^{-1}

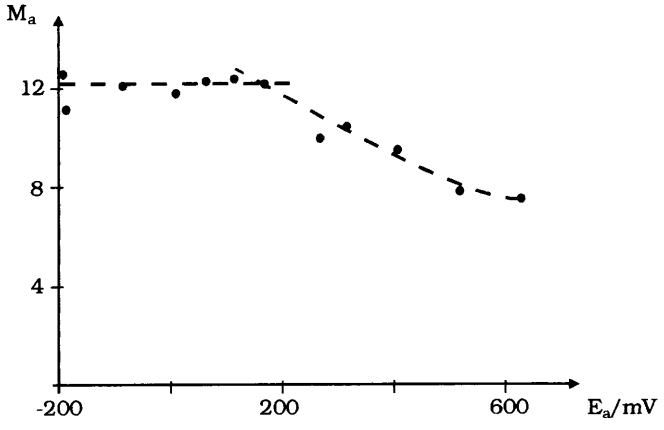

Fig. 5 Dependence of M_a values calculated for surface Pd oxide reduction on anodic potential scan limit (E_a). Solution 0.1 M KOH, scan rate 25 mV s^{-1}

various anodic potential limits, E_a, were used. Figure 5 presents the dependence of the "apparent molar mass", M_a, on the anodic potential limit of the polarization of the palladium electrode. The mass changes at the beginning of oxide formation, i.e. at potentials lower than −200 mV, were difficult to record with satisfying resolution (at the level of microbalance sensitivity) and were very irreproducible. This is the reason why only the oxides generated at potentials higher than −200 mV are discussed in this paper. In order to avoid the formation of hardly reducible β-oxides [34], the potential scan of the palladium electrode was reversed before the onset of a vigorous oxygen evolution. When the anodic potential limit, E_i, is ca. 200 mV, a change in the slope of the M_a vs. E_a plot occurs (Fig. 5), similar to the case of the Δf vs. Q_{ox} plot (Fig. 4). For lower E_a values (< 200 mV), M_a is almost constant (ca. 12.6 g mol^{-1}), while at E_a positive values of 200 mV a decrease of M_a value with the potential increase is observed. Moreover, the decrease of the M_a value with the potential increase,

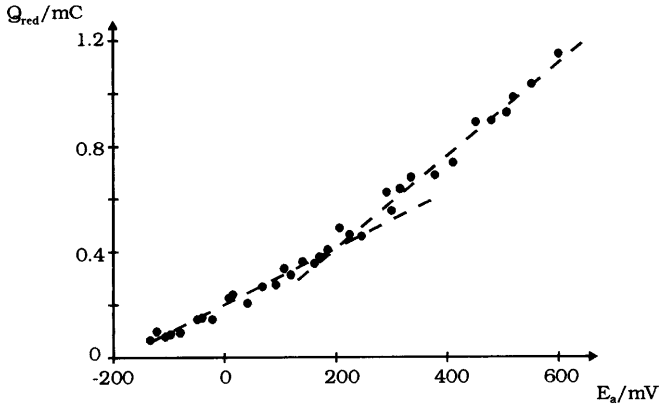

Fig. 6 Dependence of charge passed during oxide reduction (Q_{red}) on anodic potential scan limit (E_a). Solution 0.1 M KOH, scan rate 25 mV s^{-1}

observed on Fig. 5, is consistent with the decrease of the slope in the Δf vs. Q_{ox} plot (Fig. 4) for the anodic potential limit higher than E_i. These data imply that the reduction process of surface oxides is basically a reverse of the oxidation of these oxides.

Figure 6 depicts the dependence of Q_{red} on E_a. Q_{red} is the reduction charge obtained from the integration of the reduction peak observed in the potential range from ca. −150 to ca. −450 mV. As before, the change of the slope of this plot is observed at the potential value close to 200 mV. This result agrees with the data reported by Bolzán [29], who also observed the change in the slope of a Q_{red} vs. E_a plot at a similar potential. According to the interpretation proposed in that paper, this slope change is caused by the onset of Pd(IV) oxide formation.

According to the literature [35], during the early stages of the oxidation of the surface of noble metals, OH adspecies are participating in the formation of $M(OH)_n$ species. The participation of OH adspecies in the early stages of surface oxidation is also postulated by many authors for palladium electrodes in solutions with different pH values [29, 31, 36–48]. Two structures for the surface Pd(II) oxide might be considered with respect to the M_a values obtained from the EQCMB experiments: $Pd(OH)_n$ ($n = 1$ or 2) with apparent molar mass $M_a = 17$ g mol^{-1} and PdO with $M_a = 8$ g mol^{-1}.

M_a values obtained in our experiments, at potentials below 200 mV, are higher than predicted for the PdO form, but they are lower than the M_a values expected for the $Pd(OH)_n$ form. If we assume, in agreement with the literature data [29, 31, 36–48], that PdOH is the structure of the oxide formed in the early stages of surface oxidation, the most probable explanation for a M_a value lower than 17 g mol^{-1} is surface adsorption of OH^- anions [49], or water molecules, at potentials more negative than the surface oxidation. This would mean that during oxide reduction only a fraction of the OH adspecies is removed from the electrode surface and the rest still exists on the electrode surface as adsorbed OH^- anions. Another possibility is that simultaneously to the

oxide reduction and O adspecies removal from the electrode surface, OH^- or H_2O adsorption occurs. In both cases, the mass change of the electrode should be lower than predicted theoretically for the pure reduction reaction. However, our experiments with the EQCMB showed that at the potential region of a double layer charging from −600 mV to the potential of surface oxidation, the mass of the electrode is almost constant. This suggests that OH^- anion/H_2O molecules adsorption in this potential region is rather low or no significant changes in OH^-/H_2O molecules surface concentration occur. Therefore, it is not clear what is the coverage of the electrode surface with adsorbed OH^- anions/water molecules. Another explanation for this low M_a value is the existence of a mixture of products, i.e. the surface oxide might be expressed by the formula $x\mathrm{Pd(OH)}_n{\cdot}y\mathrm{PdO}$.

For the anodic potential limits beyond 200 mV, a decrease of the M_a value is observed. The M_a value seen in Fig. 5 reaches the value close to that predicted by the PdO formula. Clearly, the oxides formed during potential scan for E_a higher than 200 mV are more anhydrous than those obtained for lower E_a values. The slow decrease of M_a to the value of 8 g mol^{-1} shows that the $\mathrm{Pd(OH)}_n$ form is still participating in the oxide structure, but the relative amount of this form decreases with the E_a increase.

The effect described above might be explained as follows:

1. According to the literature data [35, 38], we propose that, simultaneously to further oxide formation, which causes the mass increase, also the disproportionation of the existing oxide occurs. This disproportionation reaction leads to the mass decrease without charge transfer, according to the following scheme:

   $$2\mathrm{MOH} \rightarrow \mathrm{M} + \mathrm{MO} + \mathrm{H_2O}$$

2. An additional layer of Pd oxide might be formed. According to the data obtained in this work from oxide reduction, this layer of oxide is more anhydrous, i.e. might be described using the PdO formula. It should be noted that the amount of the oxide formed during potentiodynamic experiments (CV) depends on the scan rate. The number of apparent oxide layers increases with the decrease of the scan rate [50].
3. According to the literature data [29], a higher oxidation state of the Pd oxide, i.e. anhydrous Pd(IV) oxide, might be formed. It has been strongly suggested that at the electrode potentials close to oxygen evolution both in basic [49, 51, 52] and in acidic solutions [31, 39, 50, 53, 54], except for the Pd(II) oxide, some amount of the Pd(IV) oxide is generated on the palladium surface. According to the literature [29, 36], the formation of Pd(IV) oxide starts at a potential close to 200 mV (vs. SCE). The changes of the "apparent molar mass", obtained in the experiments presented in this work, suggest that the reduced oxide has a mixed composition, i.e. contains both anhydrous Pd(IV) and hydrous Pd(II) oxides.

The surface oxide that is reduced in a wide, and not well defined, peak in the potential range from 300 to 0 mV is described in the literature [26, 29, 49, 51, 52, 55] as Pd(IV) oxide. The reduction peak at ca. +250 mV is observed only for $E_a \geq 480$ mV. This means that the processes that occur at potentials below 480 mV are not affected by the formation of this oxide. According to the M_a values obtained for this oxide ($M_a \approx 18$ g mol^{-1}), we can conclude that its structure is more hydrous than the structure of the oxides reduced in the main reduction peak in the potential range from ca. −150 to ca. −450 mV. This conclusion is in agreement with the data reported by Bolzán [29]. If we assume that Pd(IV) oxide is reduced not to the metallic Pd [29, 37, 52, 56] but to the anhydrous Pd(II) oxide (M_a values obtained from reduction peak at potential range from ca. −150 to ca. −450 mV for $E_a > 480$ mV are close to 8 g mol^{-1}), the formula of this oxide might be than expressed as $\mathrm{PdO(OH)_2}$ or $\mathrm{PdO_2{\cdot}H_2O}$.

Conclusions

1. A non-linear dependence between the mass change and the charge consumed during hydrogen oxidation in the palladium electrode was found. For this reason, the calculation of the amount of absorbed hydrogen from the EQCMB data is very doubtful.
2. The change in the structure of surface palladium oxides is observed at a potential of ca. 200 mV. It seems that the first stage of surface oxidation is related to the generation of OH adspecies. Surface oxides formed at higher anodic potentials seem to be more anhydrous. At potentials beyond 480 mV, another form of the oxide is formed and it is reduced in a very broad current peak in the potential range from 300 to 0 mV. The structure of this oxide is more hydrous than the structure of oxides reduced in the main reduction peak at ca. −300 mV.
3. Palladium dissolution in basic solutions is much lower than that observed in acidic solutions.

Acknowledgements This work was financially supported by the Polish State Committee for Scientific Research (KBN) grant no. 3T09A 052 13.

References

1. Bucur RV, Flanagan TB (1974) Z Phys Chem NF 88: 225
2. Bucur RV, Mecea V, Flanagan TB (1976) Surf Sci 54: 477
3. Frazier GA, Glosser R (1979) J Phys D Appl Phys 12: L113
4. Frazier GA, Glosser R (1980) J Less-Common Met 74: 89
5. Lee MW, Glosser R (1985) J Appl Phys 57: 5236

6. Cheek GT, O'Grady WE (1990) J Electroanal Chem 277: 341
7. Gräsjo L, Seo M (1990) J Electroanal Chem 296: 233
8. Yamamoto N, Ohsaka T, Terashima T, Oyama N (1990) J Electroanal Chem 296: 463
9. Oyama N, Yamamoto N, Hatozaki O, Ohsaka T (1990) Jpn J Appl Phys 29: L818
10. Cheek GT, O'Grady WE (1994) J Electroanal Chem 368: 133
11. Grdeń M, Kotowski J, Czerwiński A (1999) J Solid State Electrochem 3: 348
12. Rand DAJ, Woods R (1972) J Electroanal Chem 35: 209
13. Czerwiński A, Marassi R (1992) J Electroanal Chem 322: 373
14. Czerwiński A, Maruszczak G, Żelazowska M, Łańcucka M, Marassi R, Zamponi S (1995) J Electroanal Chem 386: 207
15. Czerwiński A, Czauderna M, Maruszczak G, Kiersztyn I, Marassi R, Zamponi S (1997) Electrochim Acta 42: 81
16. Czerwiński A, Zamponi S, Marassi R (1991) J Electroanal Chem 316: 211
17. Czerwiński A (1995) Pol J Chem 69: 699
18. Koh W, Kutner W, Jones MT, Kadish KM (1993) Electroanalysis 5: 209
19. Hoare JP, Schuldiner S (1957) J Phys Chem 61: 399
20. Flanagan TB, Lewis FA (1959) Trans Faraday Soc 55: 1409
21. Burshteyn RH, Vilinskaya VS, Tarasevich MR (1969) Elektrokhimiya 12: 1861
22. Czerwiński A (1994) Electrochim Acta 39: 431
23. Czerwiński A, Frydrych J, Kiersztyn I (1996) Anal Lett 29: 2549
24. Enyo M, Biswas P (1992) J Electroanal Chem 335: 309
25. Yamazaki O, Yoshitake H, Kamiya N, Ota K (1995) J Electroanal Chem 390: 127
26. Jeong MC, Pyun CH, Yeo IH (1993) J Electrochem Soc 140: 1986
27. Burke LD, Casey JK (1993) J Appl Electrochem 23: 573
28. Hu CC, Wen TC (1995) J Electrochem Soc 142: 1376
29. Bolzán AE (1995) J Electroanal Chem 380: 127
30. Llopis JF, Gamboa JM, Victori L (1972) Electrochim Acta 17: 2225
31. Seo M, Aomi M (1992) J Electrochem Soc 139: 1087
32. Breiter MW (1962) J Electrochem Soc 109: 42
33. Breiter MW (1977) J Electroanal Chem 81: 275
34. Burke LD, McCarthy MM, Roche MBC (1984) J Electroanal Chem 167: 291
35. Bagotzky VS, Tarasevich MR (1979) J Electroanal Chem 101: 1
36. Hickling A, Vrjosek GG (1961) Trans Faraday Soc 57: 123
37. Hu CC, Wen TC (1996) Electrochim Acta 41: 1505
38. Gossner K, Mizera E (1981) J Electroanal Chem 125: 347
39. Bolzán AE, Martins ME, Arvía AJ (1984) J Electroanal Chem 172: 221
40. Chierchie T, Mayer C, Lorenz WJ (1982) J Electroanal Chem 135: 211
41. Bolzán AE, Chialvo AC, Arvia AJ (1984) J Electroanal Chem 179: 71
42. Perdriel CL, Custidiano E, Arvia AJ (1988) J Electroanal Chem 246: 165
43. Bolzán AE, Arvia AJ (1992) J Electroanal Chem 322: 247
44. El Wakkad SES, Shams El Din AM (1954) J Chem Soc 3094
45. Chang CC, Wen TC, Tien HJ (1997) Electrochim Acta 42: 557
46. Kim KS, Gossman AF, Winograd N (1974) Anal Chem 46: 197
47. Hu CC, Wen TC (1994) Electrochim Acta 39: 2763
48. Burke LD, Casey JK (1993) J Electrochem Soc 140: 1292
49. Zhang AJ, Birss VI, Vanýsek P (1994) J Electroanal Chem 378: 63
50. Gromyko VA (1971) Elektrokhimiya 7: 885
51. Birss VI, Beck VH, Zhang AJ, Vanýsek P (1997) J Electroanal Chem 429: 175
52. Zhang AJ, Gaur M, Birss VI (1995) J Electroanal Chem 389: 149
53. Burshteyn RH, Tarasevich MR, Vilinskaya VS (1967) Elektrokhimiya 3: 349
54. Solomun T (1988) J Electroanal Chem 255: 163
55. Chausse V, Regull P, Victori L (1987) J Electroanal Chem 238: 115
56. Kinoshita E, Ingman F, Edwall G, Glab S (1986) Electrochim Acta 31: 29